

# Study on the Quantum Confinement of Photo-Generated Carriers in Quantum Wells

Ding Ding, Weiye Liu, Jiaping Guo, Xinhui Tan, Wei Zhang, Lili Han, Zhaowei Wang<sup>✉</sup>, Weihua Gong, and Xiansheng Tang<sup>✉</sup>

**Abstract**—According to the classical theory, multi-quantum wells (MQWs) have quantum confinement effect on photo-generated carriers, which limits its application in light-to-electric devices. However, relevant experiments showed that a large proportion of photo-generated carriers can escape from MQWs sandwiched in the p-type layer and n-type layer (PIN structure), but not in the NIN structure. In order to study this phenomenon carefully, we applied positive and negative bias to an NIN structure respectively to simulate the PIN structure. By analyzing the photoluminescence (PL) spectra, we observed a weak escape behavior of photon-generated carriers among QWs in NIN structure. The experiment results indicate that strong electric field could drive carriers to escape from QWs rather than relaxation and recombination, while in NIN structure the inhomogeneous distribution of the electric field intensity reduces the carrier transport efficiency. The further study will give new ideas to design and produce photoelectric devices.

**Index Terms**—Escape, multi-quantum wells, NIN structure.

## I. INTRODUCTION

QWs are widely used in various electric-to-light devices, such as light emitting diodes (LEDs) [1], [2] and lasers diodes (LDs) [3], [4] due to their quantum confinement effect. Semiconductor quantum confinement effect usually studies semiconductor special transport of carriers in MQWs materials.

The longitudinal transport is affected by the quantum confinement effect, which is quite different from that in the horizontal direction [5]. In the light-to-electric situation, according to classical theory [5], carriers would relax to the ground state and be

confined in low dimension materials due to the quantum effect, which is beneficial to recombination for injection carriers [6], [7], [8], [9]. So MQWs is hard to be used in light-to-electric devices due to the low escape rate. But relevant experiments demonstrated an obvious carriers escape phenomenon in PIN structure (an intrinsic layer sandwiched in the p-type and n-type layer) with MQWs [10], [11], [12], [13], [14], [15], where the carriers break the quantum confinement and the escape proportion can be up to 90 percent, which is too high to be explained by thermal-electron emission and tunneling theory [5], [19], [20]. These results implies that the MQWs in PIN structure could be used in light-to-electric devices, such as solar cells [16], [17] and photodetectors [10], [18].

By applying a voltage across the NIN structure, an approximately uniform electric field can be created in the MQWs. However, in NIN structure with bias [13], [14], it's reported that there is still no phenomenon of carriers escape, which is consistent with the calculation [21]. The difference between NIN structure and PIN structure lies in whether the built-in electric fields of the two structures are evenly distributed. In this paper, we fabricated an NIN structure (an intrinsic layer sandwiched in double n-type layers) with two types of QWs to further investigate this phenomenon. By applying bias in NIN structure and analyzing the photoluminescence (PL) spectra we demonstrate how and when the photon-generated carriers will transfer among the QWs, which helps us to have a better understanding of carrier transport behavior in solar cells and photodetectors.

## II. EXPERIMENTAL DETAILS

In this work, two different samples were grown by solid source molecular beam epitaxy (SSMBE, VG V80). The structures of sample A and sample B can be seen from Fig. 1. As we can see from Fig. 1(a), sample A is a PIN structure with two-types QWs grown on n-GaAs (100) substrate ( $3e18 \text{ cm}^{-3}$ ). The intrinsic layer is the MQWs regions, including 10-pairs Al<sub>0.3</sub>Ga<sub>0.7</sub>As/In<sub>0.1</sub>Ga<sub>0.9</sub>As QWs and 10-pairs Al<sub>0.3</sub>Ga<sub>0.7</sub>As/In<sub>0.15</sub>Ga<sub>0.85</sub>As QWs. The widths of the barriers and wells are 20 nm and 5 nm respectively. The intrinsic layer is sandwiched between a 300 nm n-type Al<sub>0.3</sub>Ga<sub>0.7</sub>As layer with a doping density of  $5e17 \text{ cm}^{-3}$  and a 150 nm p-type Al<sub>0.3</sub>Ga<sub>0.7</sub>As layer with a doping density of  $5e17 \text{ cm}^{-3}$ . And then 150 nm

Manuscript received 16 March 2023; revised 17 April 2023; accepted 18 April 2023. Date of publication 21 April 2023; date of current version 2 May 2023. This work was supported by in part by the National Key research and development Program under Grant 2021YFB3201904, in part by the National Natural Science Foundation of China under Grant 62005138, in part by the Qilu University of Technology (Shandong Academy of Sciences) Peixin fund project under Grant 2022PX080, in part by the Qilu University of Technology (Shandong Academy of Sciences) International Cooperation Projects under Grant 2022GH001, in part by the Qilu University of Technology (Shandong Academy of Sciences) Computer Science and Technology “Four Plans” talent introduction and Multiplication plan project under Grant 2021YY01002, in part by the Youth fund of the Shandong Natural Science Foundation under Grants ZR2020QF098 and ZR2022QF115, and in part by the Project of Jinan under Grant 202228032. (Corresponding author: Xiansheng Tang.)

The authors are with the Laser Institute, Qilu University of Technology (Shandong Academy of Sciences), Jinan 250014, China (e-mail: 2782750211@qq.com; 2966745661@qq.com; 2900633878@qq.com; 3327467428@qq.com; zhang.wei@qlu.edu.cn; lilihan@qlu.edu.cn; zw.wang@qlu.edu.cn; weihua.gong@sdlaser.cn; 18811681359@163.com).

Digital Object Identifier 10.1109/JPHOT.2023.3269082

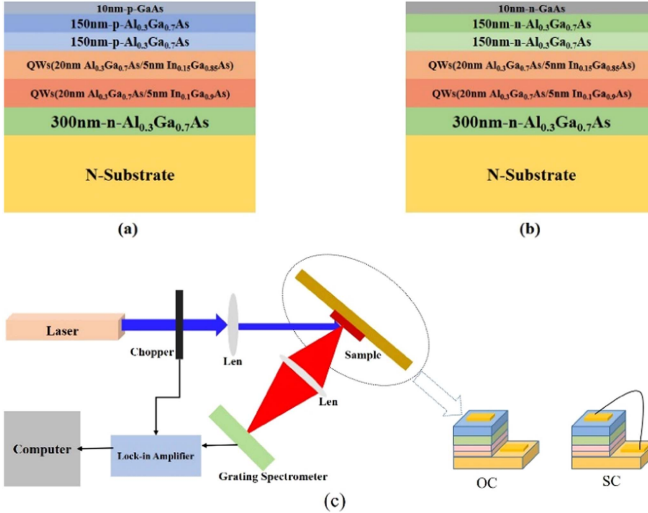


Fig. 1. (a) The schematic diagram of the PIN structure; (b) The schematic diagram of the NIN structure; (c) Schematic of the PL measurement.

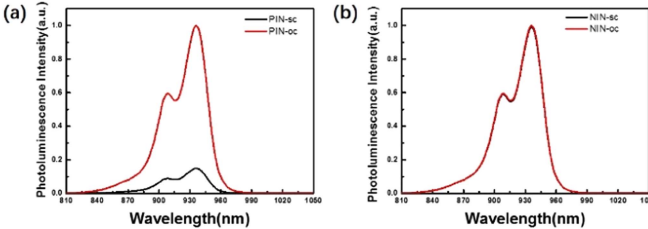


Fig. 2. (a) The PL spectra of PIN structure under short circuit and open circuit; (b) The PL spectra of NIN structure under short circuit and open circuit.

p-type Al<sub>0.3</sub>Ga<sub>0.7</sub>As layer with a doping density of  $3 \times 10^{18} \text{ cm}^{-3}$  and 10 nm p-type GaAs layer with a doping density of  $4 \times 10^{18} \text{ cm}^{-3}$  were deposited. As we can see from Fig. 1(b), sample B has the similar structure but the p-type layers were replaced by a 150 nm n-type Al<sub>0.3</sub>Ga<sub>0.7</sub>As layer with a doping density of  $5 \times 10^{17} \text{ cm}^{-3}$  and a 150 nm n-type Al<sub>0.3</sub>Ga<sub>0.7</sub>As layer with a doping density of  $3 \times 10^{18} \text{ cm}^{-3}$  and 10 nm n-type GaAs layer with doping density of  $4 \times 10^{18} \text{ cm}^{-3}$ .

To investigate the PL characteristics with bias, devices with top and bottom electrodes were fabricated. Photolithography and wet etching were used to achieve mesa isolation. Using electron beam evaporation, 20/100 nm Ti/Au were deposited in sequence to form p-ohmic contact, and 15/101/26/26/100 nm Ni/Au/Ge/Ni/Au layers were deposited to form n-ohmic contact. And Fig. 1(c) shows the schematic of the PL measurement.

### III. RESULTS

Fig. 2 shows the PL spectra of PIN structure and NIN structure under open circuit and short circuit. The wavelength of the exciting light is 730 nm and it is resonance excitation which means that photo-generated carriers only generated in quantum wells. We know that non-radiative recombination mainly comes from recombination caused by defects and Auger recombination. Because the incident light power in the test process is small

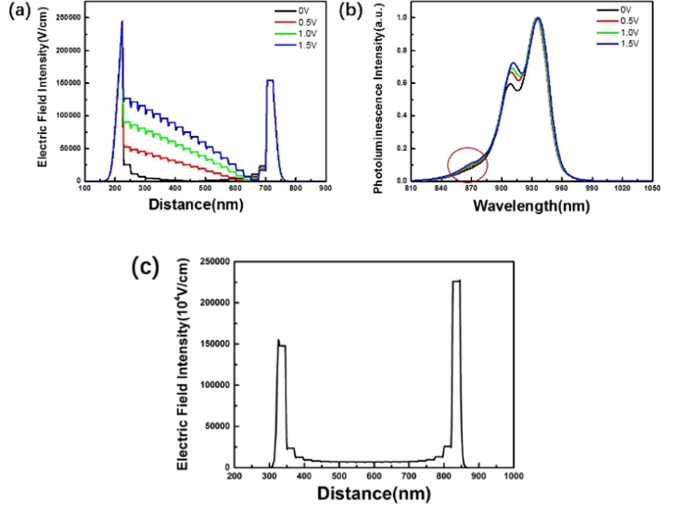


Fig. 3. (a) The electric field intensity distribution of NIN structure with bias; (b) The fluorescence spectra of NIN structure with bias. The small peak indicated by the red circle may be caused by GaAs material; (c) The electric field intensity distribution of PIN structure.

TABLE I  
THE RATIO OF SHORT-WAVE PEAK VALUE TO LONG-WAVE PEAK VALUE

Bias (V)	0	0.5	1.0	1.5
Ratio	0.596	0.666	0.690	0.726

and constant, the number of photo-generated carriers excited by it is limited, and the non-radiative recombination can be regarded as a unified background. For the convenience of subsequent analysis, we chose to ignore its non-radiative recombination. Therefore, the photogenerated carriers mainly participate in the radiative recombination, and the fluorescence intensity is proportional to the photogenerated carriers. As we can see from Fig. 2(a), there are more than 80% of carriers can escape from QWs in PIN structure under short circuit (sc), compared with the integral strength of PL under open circuit (oc), while no carriers escape from QWs in the NIN structure under short circuit from Fig. 2(b), which is consistent with the previous experimental studies. Furthermore, there are two peaks (910 nm and 935 nm) in the spectra, corresponding to the two types of QWs.

To simulate the situation of PIN structure by NIN structure, we applied positive bias (from the top surface to the substrate) to the NIN structure. As we can see from Fig. 3 and Table I, there is an obvious phenomenon of carrier transport. Fig. 3(a) shows the variation of electric field strength with applied bias. And Fig. 3(c) shows the electric field intensity distribution of PIN structure for comparison. Because the NIN structure is almost symmetrical, there are two built-in electric fields which points from the center of the QWs region to both sides. When the bias is applied, the electric field at one end is enhanced while the electric field at the other end is weakened. However, the external field can't change the directions of the two electric fields inside. Fig. 3(b) shows the variation of PL spectra with different bias.

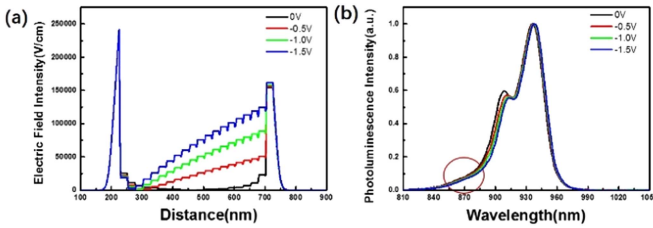


Fig. 4. (a) The electric field intensity distribution of NIN structure with bias; (b) The fluorescence spectra of NIN structure with bias. There is no small peak in the red circle.

TABLE II  
THE RATIO OF SHORT-WAVE PEAK VALUE TO LONG-WAVE PEAK VALUE

Bias (V)	0	-0.5	-1.0	-1.5
Ratio	0.596	0.572	0.562	0.555

It is found that the long-wave peak shifts to the short-wave peak position with the increase of bias voltage, showing that the carriers in the wells corresponding to the long-wave peak transfer to the wells corresponding to the short-wave peak. It can be known that the phenomenon of photo-generated carriers escape gets more obvious with the bias or electric field intensity increasing. Table I shows the ratio of short-wave peak intensity to long-wave peak intensity under different bias. And it is can be seen that the ratio is 0.596 when the bias is zero. The ratio increases to 0.726 when the bias is 1.5 V. In this part, there is a hypothesis that the change of external electric field will not change the recombination efficiency of each QW, so the fluorescence intensity can still represent the carrier distribution in the QW [21]. From Fig. 3(b), we can also see that with the increase of bias voltage, the small peak near 870 nm is gradually obvious, which is out of our expectation. We assume that the source of this peak may be due to the precipitation of very little In component in the bottom QWs because of the long heating time, which leads to the appearance of GaAs material. Because the material is at the bottom of the structure, the excited PL peak intensity is too weak to display at the beginning, and then the PL intensity becomes stronger due to the carrier injection from other QWs under the strong electric field, which can reflect the transport of carriers more clearly.

Furthermore, to explain the phenomenon more clearly, then we applied negative bias (from the top surface to the substrate) to the same NIN structure. Fig. 4(a) shows the variation of electric field strength with applied bias, which is similar with Fig. 3(a). Fig. 4(b) shows the variation of PL spectra with bias. It shows that the short-wave peak shifts to the long-wave peak position with the increase of bias voltage, which indicates that the carriers escape from the lower wells to the upper wells under bias voltage. The phenomenon of photo-generated carriers escape gets more obvious with the increasing electric field intensity. Table II also can give visualized data by showing the ratio of short-wave peak value to long-wave peak value. And we can see that the ratio is 0.596 when the bias is zero, which decreases to 0.555 when the

bias is -1.5 V. From Fig. 4(b), with the increase of bias voltage, there is no small peak near 870 nm, which is different from the phenomenon in Fig. 3(b). Since the bias applied is opposite, the photo-generated carriers move in the opposite direction, and there will be no excess photo-generated carriers injection in the InGaAs QW at the bottom of the structure, so its PL peak will not appear.

By applying a bias to the NIN structure to simulate the PIN structure, it's observed that the photo-generated carriers can move from wells to wells but the escape efficiency is very low compared to PIN structure. There is an intrinsic difference for the distribution of electric field intensity between a PIN structure and a NIN structure. The electric field intensity is uniform in PIN structure so all carriers are affected conformably. On the other hand, the electric field intensity is not uniform in NIN structure with bias and there is also the region in which electric field intensity is zero, consequently only these carriers located in the strong enough electric field can be affected to participate in drift. This could be the reason why 80% of photo-generated carriers can escape from QWs in PIN structure to the external circuit and the small part photo-generated carriers can escape from QWs in NIN structure with bias. The results also give strong evidence of photo-generated carriers escape with high enough electric field intensity. We believe this phenomenon is caused by the competition of escape process and recombination. It's known that the escape time is on the femtosecond scale considering the drift speed and the quantum well dimension, which is far less than the recombination time (on the nanosecond scale [22]). So photo-generated carriers are more likely to escape before recombination. The deeper mechanism of the escape phenomenon, such as the modulation function of the PN junction, is worthy of further studies.

#### IV. CONCLUSION

In conclusion, by preparing NIN structure with two types of MQWs and applying a positive and negative bias to the NIN structure respectively to simulate the PIN structure, we found that photo-generated carriers can escape from some QWs in NIN structure with bias by analyzing the PL spectra, which removes the quantum confinement effect. With the change of applied bias voltage, the peak to peak ratio of bimodal is changing, showing that carriers can escape from some QWs, but the escape rate is much lower than PIN structure. By analyzing the electric field distribution, we think this phenomenon comes from the effect of the built-in field by continuing to analyze the electric field intensity distribution in NIN structure with bias. High enough electric field intensity would drive carriers to escape which is a faster process rather than relaxation and recombination. Therefore, we think that in PIN structure, photo-generated carriers will drift out of the MQWs region preferentially instead of recombination, and the time of drift out is much shorter than that of recombination. The carrier takes priority to the faster process, which makes the quantum confinement effect not work in the PIN structure. The further study of carrier escape in MQWs will give new ideas to design and produce photoelectric devices.

## REFERENCES

- [1] H. W. Choi et al., "GaN micro-light-emitting diode arrays with monolithically integrated sapphire microlenses," *Appl. Phys. Lett.*, vol. 84, no. 13, pp. 2253–2255, 2004.
- [2] T. Nishida, H. Saito, and N. Kobayashi, "Efficient and high-power AlGaN-based ultraviolet light-emitting diode grown on bulk GaN," *Appl. Phys. Lett.*, vol. 79, no. 6, pp. 711–712, 2001.
- [3] A. N. Al-Omari et al., "Improved performance of top-emitting oxide-confined polyimide-planarized 980 nm VCSELs with copper-plated heat sinks," *J. Phys. D, Appl. Phys.*, vol. 45, no. 50, 2012, Art. no. 505101.
- [4] F. Koyama, "Recent advances of VCSEL Photonics," *J. Lightw. Technol.*, vol. 24, no. 12, pp. 4502–4513, Dec. 2006.
- [5] M. Grundmann, "The physics of semiconductors," Springer, pp. 599–651, 2006.
- [6] L. Kwac et al., "Effect of GaP barrier on efficiency enhancement of 860-nm vertical-cavity surface-emitting laser," *Infrared Phys. Technol.*, vol. 96, pp. 61–67, 2019.
- [7] P. Moser, J. A. Lott, G. Larisch, and D. Bimberg, "Impact of the oxide-aperture diameter on the energy efficiency, bandwidth, and temperature stability of 980-nm VCSELs," *J. Lightw. Technol.*, vol. 33, no. 4, pp. 825–831, Feb. 2015.
- [8] M. - K. Lee, C. - L. Ho, and C.-H. Fan, "Enhancement of light extraction efficiency of gallium nitride flip-chip light-emitting diode with silicon oxide hemispherical microlens on its back," *IEEE Photon. Technol. Lett.*, vol. 20, no. 15, pp. 1293–1295, Aug. 2008.
- [9] H. Guo et al., "High-performance GaN-based light-emitting diodes on patterned sapphire substrate with a novel patterned SiO<sub>2</sub>/Al<sub>2</sub>O<sub>3</sub> passivation layer," *Appl. Phys. Exp.*, vol. 6, no. 7, 2013, Art. no. 72103.
- [10] J. Liu et al., "InAs/InGaAs/InAlAs interband quantum well infrared photodetector (IQWIP) with cut-off response wavelength at 1.93 μm," *Appl. Phys. Exp.*, vol. 12, no. 3, 2019, Art. no. 32005.
- [11] Y. Li et al., "Visualizing light-to-electricity conversion process in InGaN/GaN multi-quantum wells with a p–n junction," *Chin. Phys. B.*, vol. 27, no. 9, 2018, Art. no. 97104.
- [12] H. Yang et al., "The enhanced photo absorption and carrier transportation of InGaN/GaN quantum wells for photodiode detector applications," *Sci. Rep.*, vol. 7, no. 1, 2017, Art. no. 43357.
- [13] H. Wu et al., "Direct observation of the carrier transport process in InGaN quantum wells with a pn-junction," *Chin. Phys. B.*, vol. 25, no. 11, 2016, Art. no. 117803.
- [14] W. Wang et al., "Carrier transport in III–V quantum-dot structures for solar cells or photodetectors," *Chin. Phys. B*, vol. 25, no. 9, pp. 174–179, 2016.
- [15] S. Lim, Y. -H. Ko, and Y. H. Cho, "A quantitative method for determination of carrier escape efficiency in GaN-based light-emitting diodes: A comparison of open- and short-circuit photoluminescence," *Appl. Phys. Lett.*, vol. 104, no. 9, 2014, Art. no. 91104.
- [16] J. R. Lang et al., "Carrier escape mechanism dependence on barrier thickness and temperature in InGaN quantum well solar cells," *Appl. Phys. Lett.*, vol. 101, no. 18, 2012, Art. no. 181105.
- [17] A. Luque, A. Martí, and C. Stanley, "Understanding intermediate-band solar cells," *Nature Photon.*, vol. 6, no. 3, pp. 146–152, 2012.
- [18] B. F. Levine, "Quantum-well infrared photodetectors," *J. Appl. Phys.*, vol. 74, no. 8, pp. R1–R81, 1993.
- [19] M. Gurioli et al., "Thermal escape of carriers out of GaAs/Al<sub>x</sub>Ga<sub>1-x</sub>As quantum-well structures," *Phys. Rev.*, vol. 46, no. 11, pp. 6922–6927, 1992.
- [20] D. J. Moss et al., "Ultrafast electron tunneling times in reverse-biased quantum-well laser structures," *Proc. SPIE*, vol. 1675, pp. 418–427, 1992.
- [21] X. Tang et al., "Research on photo-generated carriers escape in PIN and NIN structures with quantum wells," *Appl. Phys. Exp.*, vol. 13, no. 7, 2020, Art. no. 71009.
- [22] D. Morris et al., "Electron and hole capture in multiple-quantum-well structures," *Phys. Rev. B*, vol. 47, no. 11, pp. 6819–6822, 1993.